A study of infiltration on three sand capillary barriers

Hong Yang, H. Rahardjo, E.C. Leong, and D.G. Fredlund

Abstract: The capillary barrier effect was investigated by conducting infiltration tests on three soil columns of fine sand over medium sand, medium sand over gravelly sand, and fine sand over gravelly sand. The barrier effect was verified in the underlying layer of coarser material, and the water-entry values of the coarser layers were confirmed to be nearly equal to the residual matric suctions of the soils. The coarser layer of gravelly sand, which had a lower water-entry value, was more effective in forming a barrier than the coarser layer of medium sand, which had a higher water-entry value. When the capillary barrier was comprised of a coarser layer of gravelly sand, there was more water stored in the finer layer at the end of the drying stage than when the capillary barrier was comprised of a coarser layer of medium sand. Non-equilibrium static conditions of pore-water pressure profiles were observed in the three soil columns, and a generalized ultimate pore-water pressure profile of a capillary barrier system was proposed. In addition, the final volumetric water contents versus matric suctions of the soils as measured from the soil columns were reasonably consistent with the soil-water characteristic curves (SWCCs) of the soils, suggesting that the drying SWCC of a soil could also be obtained from the drying process in a soil column (or a capillary open tube). The drying SWCC could be established from measurements in the soil column up to a height corresponding to two times the residual matric suction head of the soil.

Key words: capillary barrier, soil column, soil-water characteristic curve, pore-water pressure, water content, matric suction.

Résumé : On a étudié l'effet d'écrans capillaires en réalisant des essais d'infiltration sur trois colonnes de sols constituées de sable fin sur du sable moyen, de sable moyen sur du sable graveleux, et de sable fin sur du sable graveleux. L'effet d'écran a été vérifié dans la couche sous-jacente de matériau plus grossier et il a été confirmé que les valeurs d'entrée d'air des couches de matériau plus grossier étaient presque égales aux succions matricielles résiduelles des sols. La couche plus grossière de sable graveleux qui avait une valeur plus faible d'entrée d'air était plus efficace pour former un écran que la couche plus grossière de sable moyen qui avait une valeur d'entrée d'air plus élevée. Lorsque l'écran capillaire comprenait une couche plus grossière de sable graveleux, il y avait plus d'eau entreposée dans la couche fine à la fin du stade de dessiccation par rapport à l'écran capillaire qui était formé d'une couche plus grossière de sable moyen. On a observé les conditions statiques dans l'état transitoire de profils de pressions interstitielles dans les trois colonnes de sol et on a proposé un profil ultime généralisé de pressions interstitielles d'un système d'écran capillaire. De plus, les teneurs en eau volumétriques finales en fonction des matrices de succion des sols telles que mesurées dans les colonnes de sol sont raisonnablement en accord avec les courbes sol-eau (SWCC) caractéristiques des sols, ce qui suggère que la courbe SWCC de dessiccation d'un sol pourrait aussi être obtenue en partant du processus de dessiccation dans une colonne de sol (ou dans un tube capillaire). On peut établir la courbe SWCC de dessiccation en partant de mesures dans une colonne de sol jusqu'à une hauteur correspondant à deux fois la charge de succion matricielle résiduelle du sol.

Mots clés : écran capillaire, colonne de sol, courbe caractéristique sol-eau, pression interstitielle, teneur en eau, succion matricielle.

[Traduit par la Rédaction]

1. Introduction

A capillary barrier is an earthen cover system, usually comprising a finer grained layer of soil overlying a coarser grained layer of soil (e.g., Ross 1990; Stormont 1996). The difference in particle size of the soils in the capillary barrier results in the difference in the hydraulic properties (i.e., soil-water characteristic curves (SWCCs) and coefficients of the permeability) of the soils across the finer–coarser soil interface. With a low pore-water pressure at the soil interface un-

Received 5 September 2002. Accepted 19 February 2004. Published on the NRC Research Press Web site at http://cgj.nrc.ca on 24 August 2004.

H. Yang, H. Rahardjo,[1] and E.C. Leong. School of Civil and Environmental Engineering, Nanyang Technological University, Block N1, 1A-02, 50 Nanyang Avenue, 639798 Singapore.
D.G. Fredlund. Department of Civil Engineering, University of Saskatchewan, Saskatoon, SK S7N 5A9, Canada.

[1]Corresponding author (e-mail: chrahardjo@ntu.edu.sg).

 doi: 10.1139/T04-021 © 2004 NRC Canada

Fig. 1. Grain-size distribution of the soils.

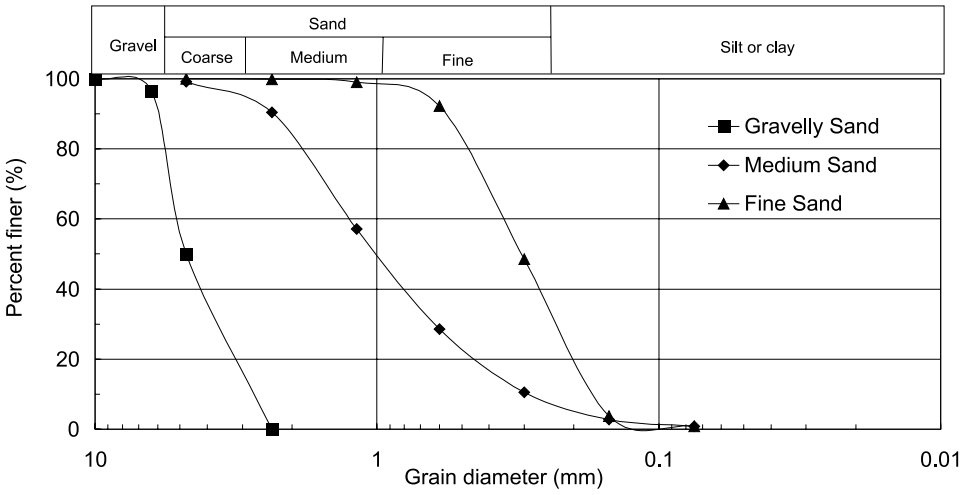

Table 1. Basic properties of the soils used in the study.

	Gravelly sand	Medium sand	Fine sand
Unified Soil Classification System	SP	SP	SP
Specific gravity, G_s	2.62	2.60	2.65
Saturated permeability, k_s (m/s)	7.6×10^{-2}	2.0×10^{-4}	2.7×10^{-4}
Dry density, ρ_d (Mg/m^3)	1.62	1.69	1.56
Void ratio, e	0.617	0.538	0.699
Porosity, n (%)	38.2	35.0	41.1
Water content at saturation, w (%)	23.6	20.7	26.4

der unsaturated conditions, the coarser grained soil layer normally has a much lower permeability than the finer grained soil layer. Therefore, the low permeability of the coarser grained layer limits the downward movement of water and holds the infiltrating water in the finer grained layer by capillary forces. The water stored temporarily in the finer grained layer is ultimately removed by evaporation and transpiration, lateral drainage (if the finer–coarser interface is on a slope), or percolation (breakthrough into the lower layer). If breakthrough occurs, the system no longer forms a barrier to the downward water movement. Applications of capillary barriers include the capping of landfills and mining wastes (e.g., Yanful et al. 1993) and the protection of slopes.

In this paper, three capillary barriers were studied by conducting infiltration tests in the laboratory on three soil columns, namely fine sand over medium sand (column FM), medium sand over gravelly sand (column MG), and fine sand over gravelly sand (column FG). The major objective of the study was to investigate the characteristics of the capillary barriers under a one-dimensional condition with a constant lower boundary during and after infiltration. The characteristics of the capillary barriers were examined by investigating the effectiveness of the barriers, the role of the water-entry values of the coarser grained layers, and the ultimate pressures in the capillary barrier system. In addition, an attempt was made to compare the water content versus matric suction of the soils at the final stage of the drying process with the soil-water characteristic curves.

2. Materials and methods

2.1. Materials and their properties

Three sands were used in the study, namely gravelly sand (GS), medium sand (MS), and fine sand (FS). The gravelly sand, crushed from fresh granite, was light grey to white in colour and was obtained commercially. It was essentially a mixture of coarse sand (50.1%) and fine gravel (49.9%). The medium sand was a light brown construction sand from a local construction site, and the fine sand was a light grey beach sand.

Classification tests were conducted on samples for each of the three soils classified according to the Unified Soil Classification System (USCS) (American Society for Testing and Materials (ASTM 1997*d*) test method D2487-93). Particle-size analyses were conducted using a sieve analysis as described in ASTM (1997*a*) test method D422-63, and the results are shown in Fig. 1. All three soils were categorized as poorly graded sands (SP in the USCS). Specific gravity tests were performed in accordance with ASTM (1997*b*) test method D854-92. The saturated permeability of the soil was investigated using the constant-head method as described in ASTM (1997*c*) test method D2434-68. The basic properties of the soils are summarized in Table 1. The dry densities of the soils were controlled to produce consistent soil properties for the saturated permeability tests, SWCC tests, and infiltration tests.

The relationship between volumetric water content and matric suction for a soil is described by an SWCC. Drying

© 2004 NRC Canada

SWCCs for the soils were obtained using a Tempe pressure plate cell (Soilmoisture Equipment Corporation 1999) by starting the tests from a saturated condition. The Tempe cell operates on the same principle as the pressure plate apparatus described in ASTM (1997*e*) test method D2325-68 (Fredlund and Rahardjo 1993). In this study, Tempe cells 88 mm in diameter and 30 mm in height (model 1405 B01M3-3) were used. Wetting SWCCs were measured using a capillary rise open tube (Fig. 2), with the soil specimen being dry initially. More details on capillary tube tests can be obtained from Lambe (1951), Lambe and Whitman (1979), and Fredlund and Rahardjo (1993).

The SWCC test data were best fit to the Fredlund and Xing (1994) equation to obtain complete drying and wetting SWCC functions for each soil. The commercially available computer software SoilVision (SoilVision Systems Ltd. 1997) was used to perform the fitting calculations. The best-fit drying and wetting SWCCs for the soils are shown in Fig. 3 (the test data and data from the soil columns are presented in Figs. 16–18 for comparison purposes), and the parameters of the SWCCs are listed in Table 2.

The Fredlund et al. (1994) prediction method was used to determine the permeability functions for the soils at different matric suctions. The method involves integrating the volumetric water content along the SWCC and requires an input of saturated permeability, k_s (as in Table 1). The drying and wetting permeability functions were predicted using the drying and wetting SWCCs, respectively. The calculations for determining the permeability functions were also performed using the SoilVision software (SoilVision Systems Ltd. 1997). The predicted permeability functions of the soils are shown in Fig. 4.

2.2. Infiltration experiments

The infiltration tests were conducted in a 190 mm internal diameter, 1 m high, transparent acrylic cylinder. A schematic diagram of the soil column apparatus is shown in Fig. 5. Columns FM, MG, and FG were constructed in the cylinders. The thickness of each soil was 500 mm. The soils were initially oven-dry and were placed at the controlled dry densities as given in Table 1. The soils were compacted in lifts with a maximum thickness of 100 mm into the acrylic cylinder with a 2.5 kg Proctor hammer by applying the same number of hammer drops for the same amount of soil. The required number of hammer drops to achieve the target density was found by carrying out trial compaction tests for each soil. On average, 20–25 drops were required for compacting one layer of 100 mm thick soil.

A tensiometer–transducer system was used in the study to monitor the pore-water pressure of the soil in the infiltration column. Small tip tensiometers (Soilmoisture Equipment Corporation 1999, catalogue no. 2100F) fitted with pressure transducers were used in the tests. The small tip tensiometer included a 1 bar (100 kPa) high-flow, high air-entry ceramic cup and a plastic body tube. The ceramic cup (Soilmoisture Equipment Corporation 1999, catalogue no. 2100F-200CR) had a round bottom 6 mm in diameter and a straight wall 25 mm in length and was attached to the tensiometer body via a coaxial polyethylene tube assembly. The ceramic cup was installed in the soil columns through a hole in the cylinder and fastened with a stainless steel connector that was mounted on the wall of the cylinder. Rubber O-rings and thread tapes were used on the connector to form a seal in the connection area to prevent leakage.

Fig. 2. Schematic diagram of the capillary rise open tube. g, gravitational acceleration; H, height; u_w, pore-water pressure; ρ_w, density of water.

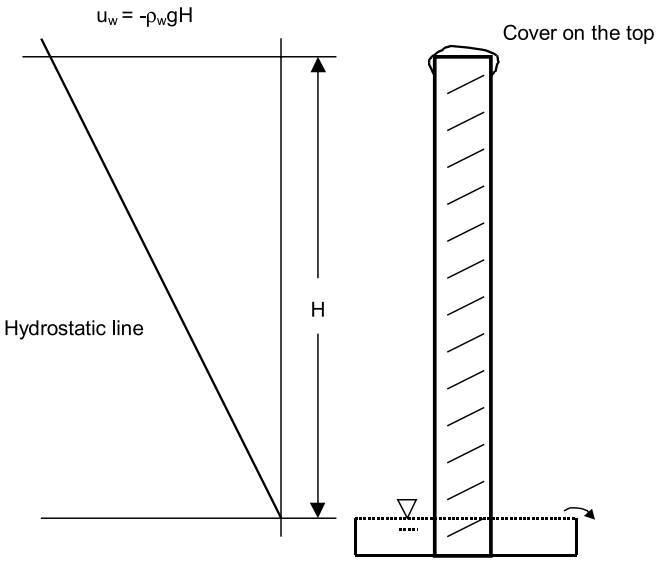

The pressure transducers were of the Kristal brand (Kistler Instrumente AG, Winterthur, Switzerland). The assembly of the tensiometer–transducer formed a seal that did not allow inflow or outflow of air under working conditions (i.e., only water was allowed to flow across the wall of the ceramic cup). The other end of the transducer was connected to a data logger (DataShuttle brand, IOtech, Inc., Cleveland, Ohio) that had an integrated AC power supply. The assemblage of the transducer and the data logger was calibrated before the infiltration tests. All the calibrations showed a linear relationship between pressure and voltage, with a linear best-fit regression R^2 value greater than 0.999. Some fluctuations in the pressure readings were observed during the tests, however. The fluctuations appeared to be caused by heat accumulated in the data logger, and consequently the performance of components of the data logger was affected. Each unit of the data logger consisted of eight differential analogue inputs (channels) and allowed eight tensiometers–transducers to be connected. The data logger was connected to a personal computer to further process the recorded data through the DASYLab communication software (IOtech, Inc., Cleveland, Ohio).

Simulated rainfall was applied to the top of the soil column through four outlets that were controlled by a regulator. The regulator controlled water flow supplied from a water tank of constant head (Fig. 5). Under the constant pressure water head, a constant rate of water flow was applied to the top of the soil column. Different flow rates were obtained by adjusting the regulator. The water flow rate was verified before and after each rainfall test. The top of the soil column was covered when no rainfall was applied to prevent evaporation.

© 2004 NRC Canada

Fig. 3. Fitted soil-water characteristic curves (SWCC) for gravelly sand (GS), medium sand (MS), and fine sand (FS).

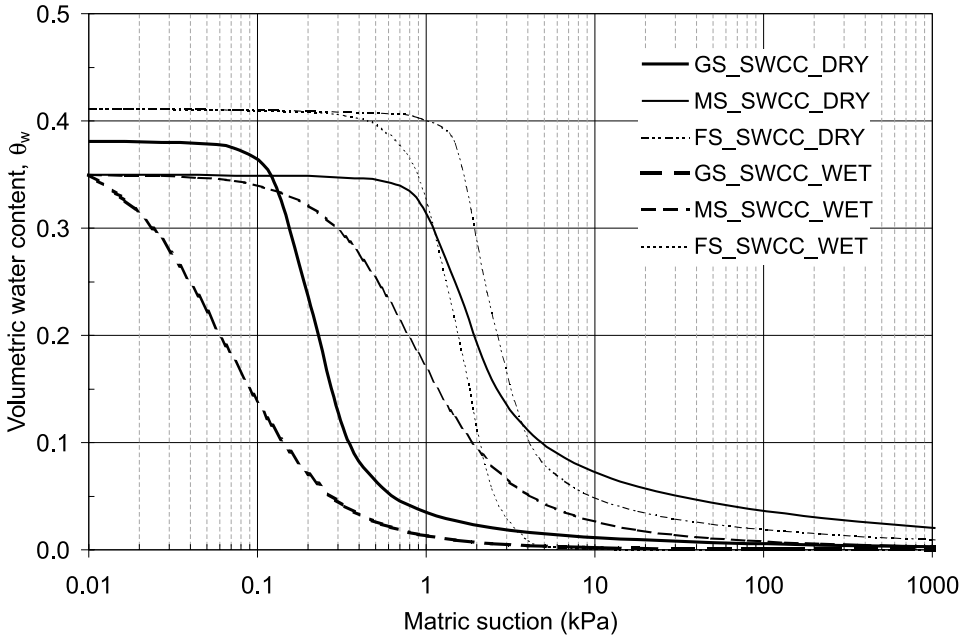

Table 2. Results of soil-water characteristic curve and Fredlund and Xing (1994) fitting parameters of the soils.

	Symbol	Gravelly sand	Medium sand	Fine sand
Drying curve				
Saturated volumetric water content	θ_s	0.382	0.350	0.411
Air-entry value (kPa)	ψ_a	0.110	0.850	1.400
Residual matric suction (kPa)	ψ_r	0.401	3.750	3.940
Residual volumetric water content	θ_r	0.0213	0.0626	0.0345
Fredlund and Xing fitting parameters	*a*	0.176	1.239	1.941
	n	4.440	4.386	6.302
	m	1.1126	0.6610	0.8680
Wetting curve				
Water-entry value (kPa)	ψ_w	0.285	3.180	2.690
Volumetric water content at ψ_w	θ_w	0.0074	0.0205	6.07×10^{-5}
Fredlund and Xing fitting parameters	*a*	0.0712	0.6770	1.8080
	n	1.232	1.620	3.193
	m	2.710	1.669	3.740

As boundary conditions are necessary for the study of infiltration behaviour (Fredlund and Rahardjo 1993), a constant lower boundary condition was formed at the bottom of the soil column by maintaining a constant water table using a large water tank. In addition, the applied rainfall that flowed through the soil column (percolation) was collected through an outlet at the bottom of the soil column and periodically weighed. The resolution of the weighing balance was 0.5 g (or 0.018 mm of water in the soil column). The drainage velocity could be calculated from the cumulative percolation amount.

After constructing the soil column, the column was saturated by allowing water to flow from the bottom of the column under a small hydraulic gradient to minimize disturbance to the soil structure. The hydraulic gradient in the finer grained soil layer (fine or medium sand) was about 0.5, which was less than the critical hydraulic gradient of the soil (about 1.0) that could cause the soil to become quick. The column was at a hydrostatic condition when the water table was maintained at the top of the column. A test that involved the rapid drawdown of the water table was then conducted by opening the valve at the bottom of the column. The purpose of the drawdown test was to establish an initial condition for the subsequent infiltration test in the soil col-

© 2004 NRC Canada

Fig. 4. Predicted permeability functions (k_w) for gravelly sand (GS), medium sand (MS), and fine sand (FS).

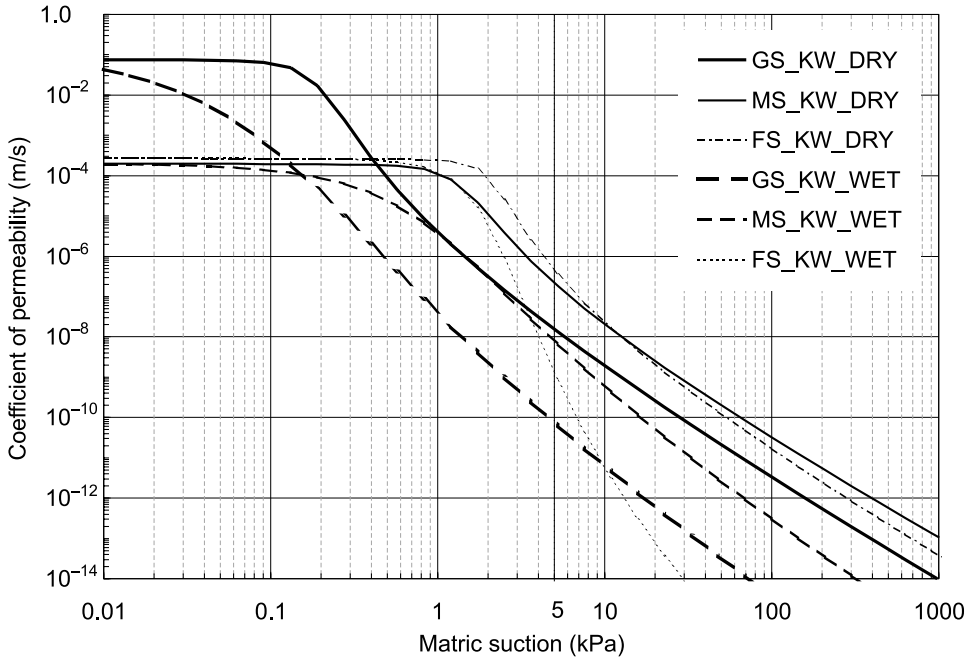

Fig. 5. Schematic diagram of the infiltration column apparatus. TDR, time-domain reflectometer.

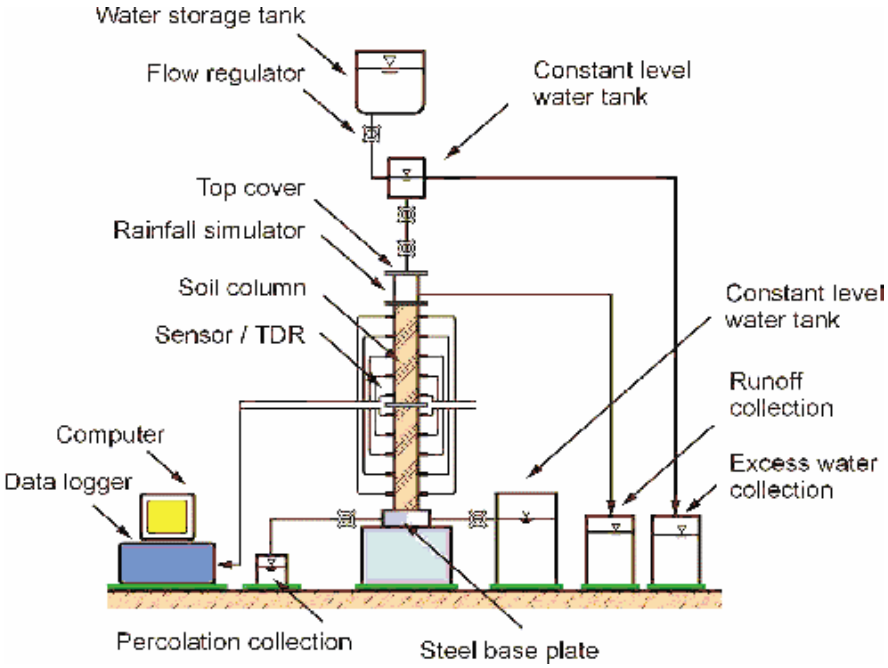

umn, as the initial condition was necessary for an infiltration study. A few days after the drawdown test, a negative pore-water pressure profile was established in the soil column and a rainfall with a specified intensity and duration (normally less than a few hours) was applied to the soil column. A second rainfall was applied a few days after the end of the first rainfall. A third rainfall was applied after the second rainfall was stopped for several days. During all the rainfall tests, the water table was maintained at the bottom of the soil column (elevation $z = 0$). At the end of each soil column test, soil samples were taken at different elevations to determine the water content of the soil by oven-drying.

3. Test results

3.1. Results from fine sand over medium sand (column FM)

A test that involved the rapid drawdown of the water table (test FM-D in Fig. 6) was performed following saturation of the soil column. A rainfall test (test FM-R1) was then con-

© 2004 NRC Canada

Fig. 6. Pore-water pressure head profiles in drawdown test in the soil column of fine sand over medium sand (test FM-D). *t*, elapsed time.

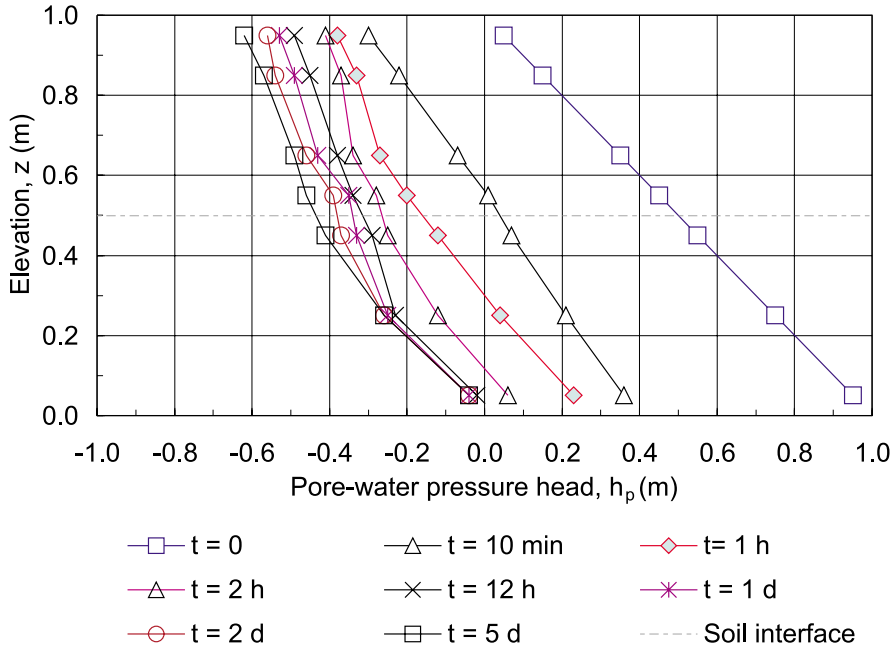

Fig. 7. Pore-water pressure head profiles in a rainfall test in the soil column of fine sand over medium sand (test FM-R2).

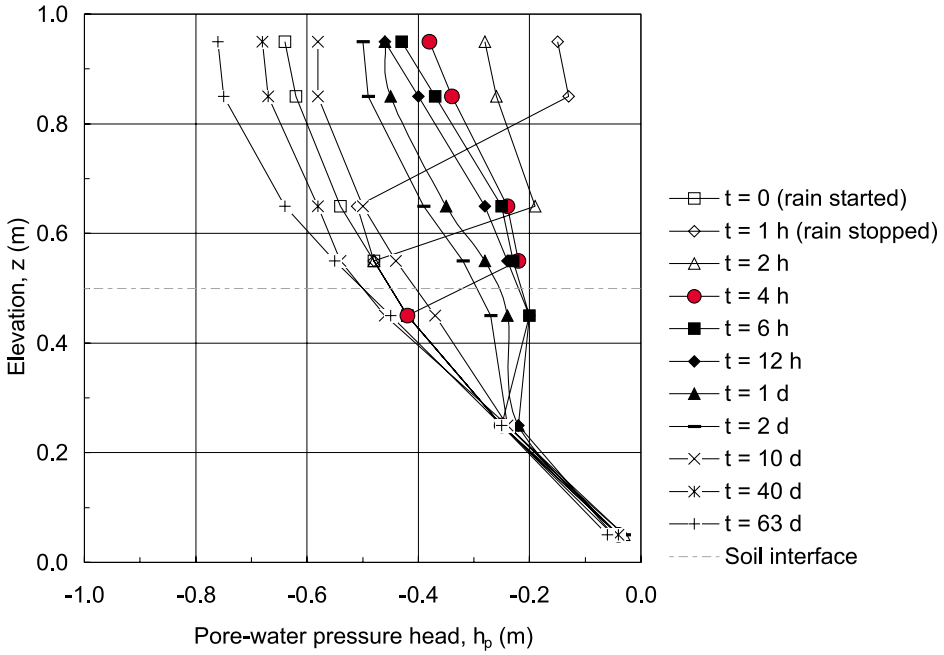

ducted 5 days later. About 20 days after test FM-R1, a second rainfall test (i.e., test FM-R2, see Fig. 7) was then conducted with a rainfall intensity of 1.1×10^{-5} m/s and a duration of 1 h, and the soil column was subsequently left for 63 days. The drainage velocity versus time for test FM-R2 is shown in Fig. 8. Water contents were measured on soil samples taken at different elevations in the soil column at the end of test FM-R2 (Fig. 9).

3.2. Results from medium sand over gravelly sand (column MG) and fine sand over gravelly sand (column FG)

A test of rapid drawdown of the water table was conducted on column MG following the saturation of the soil column (test MG-D in Fig. 10). A rainfall test (test MG-R1 in Fig. 11) was then conducted 11 days later with an applied rainfall intensity of 1.6×10^{-5} m/s and a duration of 80 min.

© 2004 NRC Canada

Fig. 8. Drainage velocity versus time in a rainfall test in the soil column of fine sand over medium sand (test FM-R2).

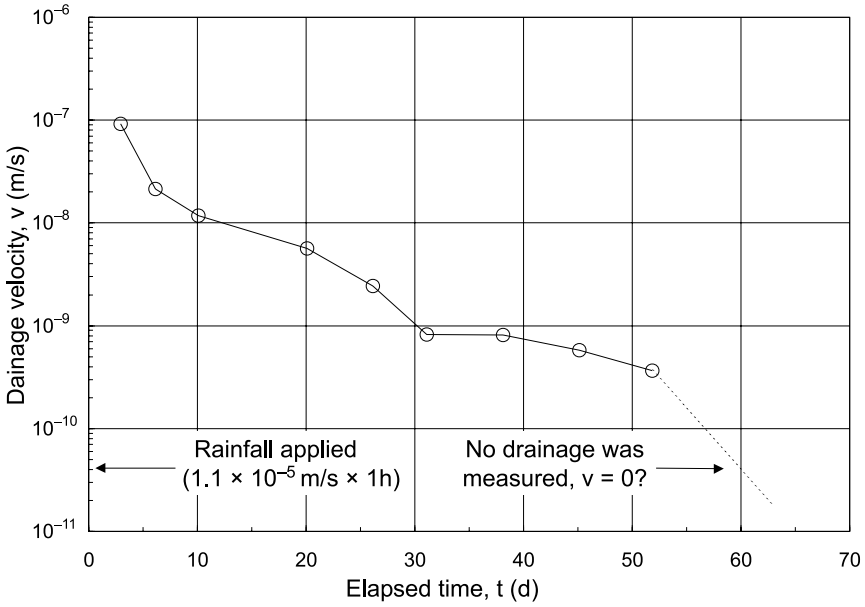

Fig. 9. Final volumetric water content in the soil column of fine sand over medium sand (at the end of test FM-R2).

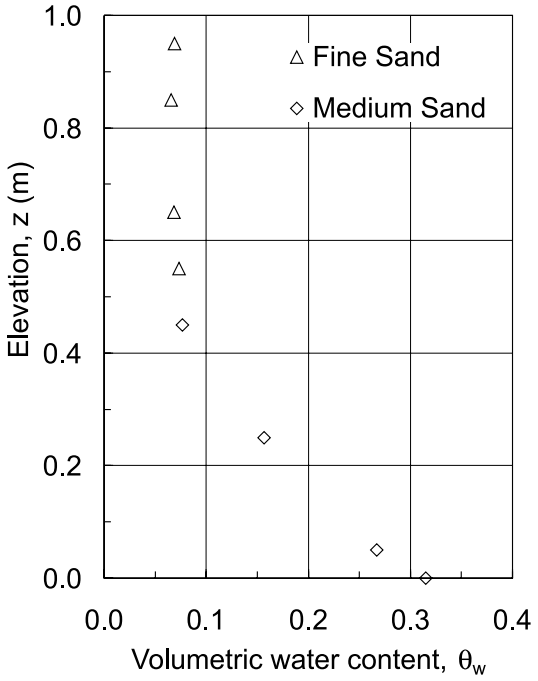

Another two rainfall tests (tests MG-R2 and MG-R3) were later conducted with different intensities and durations.

A similar test procedure was followed on column FG by conducting a drawdown test (FG-D) and three rainfall tests (tests FG-R1, FG-R2, and FG-R3). The pore-water pressure profiles were similar to those from the corresponding test results from column MG; therefore, only the pore-water pressure head profiles for the drawdown test (test FG-D) are presented in Fig. 12.

In both soil columns MG and FG, water contents were measured on soil samples at different elevations at the end of the third rainfall test (i.e., tests MG-R3 and FG-R3, which were 10 and 11 days, respectively, after the rainfall stopped). The results are shown in Fig. 13.

4. Discussion

4.1. General characteristics of the infiltration tests

In the drawdown test FM-D (Fig. 6), the pore-water pressure head profile decreased throughout the column in a relatively uniform pattern and there was no apparent difference across the finer–coarser soil interface. This behaviour could be attributed to the relatively similar coefficients of saturated permeability (k_s) and unsaturated permeability (k_w) in the fine and the medium sand in the soil column as shown in Fig. 4. The contrast between the permeabilities of the finer and coarser layers was not significant, and the soil column can be visualized as a relatively uniform column compared with the other two soil columns. It also took a relatively long time of more than 2 h to develop the negative pore-water pressures throughout the entire soil column.

In drawdown tests MG-D (Fig. 10) and FG-D (Fig. 12), the pore-water pressure head profiles were quite different from that of test FM-D. The pore-water pressure head became negative over the entire soil column almost instantaneously after the test started. It took less than 10 min to fully achieve a relatively stable negative pore-water pressure head profile in the coarser layer (i.e., the gravelly sand). Most of the subsequent changes in this layer appeared to be minor fluctuations in the readings. On the other hand, it took more than 10 days to achieve a relatively stable negative pore-water pressure head profile in the finer layers. In addition, the different rates of development of the negative pore-water pressure head profiles in the finer layer and in the coarser layer at the beginning of each test also resulted in the abrupt change in the pore-water pressure head along the finer–coarser soil interface in each of the two columns.

© 2004 NRC Canada

Fig. 10. Pore-water pressure head profiles in drawdown test in the soil column of medium sand over gravelly sand (test MG-D).

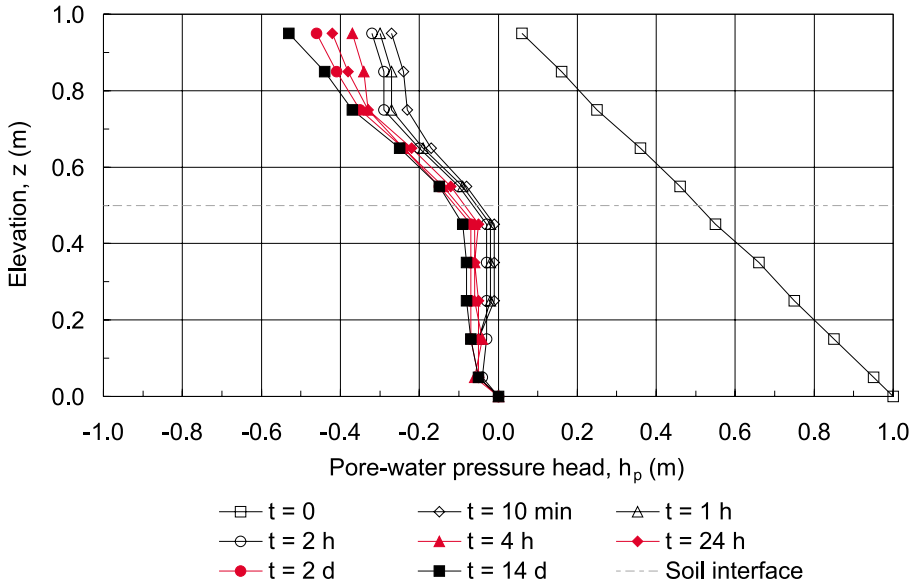

Fig. 11. Pore-water pressure head profiles in a rainfall test in the soil column of medium sand over gravelly sand (test MG-R1).

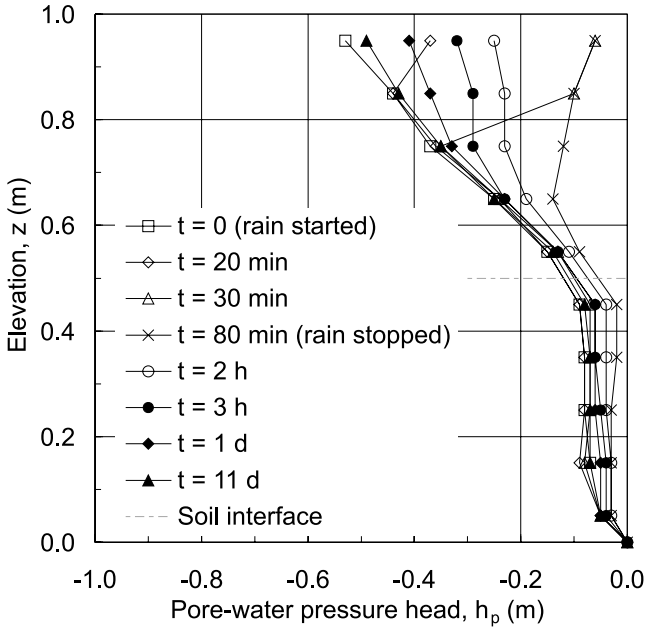

The faster development of the pore-water pressure head profiles in the coarser layer as compared to that in the finer layer can be attributed to the higher k_w of the coarser layer than that of the finer layer at low matric suctions (Fig. 4) for both soil columns. The rate of development of the negative pore-water pressure head profile in the finer layer became slower as the ultimate profile was approached in each of the three soil columns. The reason can be observed from the permeability functions in which k_w became extremely small when the matric suction increased (i.e., the pore-water pressure head decreased).

The results of the rainfall tests (test FM-R2 in Fig. 7 and test MG-R1 in Fig. 11) showed continuous changes in the pore-water pressure head, indicating the transient process of the tests. The entire transient process was also reflected in the curve of drainage rate versus time (Fig. 8 for test FM-R2). There was an increase in the drainage rate after the rainfall was applied and a subsequent decrease after the rainfall stopped. The continuous decrease in the drainage rate corresponded to the continuous decrease in the pore-water pressure head in the soil column. In test FM-R2, the weighing balance did not record any increase in the cumulative drainage starting from 52 days after the rainfall stopped. As the resolution of the weighing balance was 0.5 g, the maximum possible drainage amount that could occur during the period of 52–63 days (when the test was stopped) was 0.5 g, which was equivalent to an average drainage velocity of 1.9×10^{-11} m/s. Since this average drainage velocity was much smaller than the last recorded drainage rate of 3.6×10^{-10} m/s, it was considered that the cumulative drainage from the bottom of the soil column essentially stopped 52 days after the rainfall (Fig. 8).

The change in the pore-water pressure head for both the drying and wetting processes of the rainfall tests could be explained using the SWCCs of the soils (Fig. 3). The increase in water content during the wetting process corresponded to a decrease in matric suction (i.e., increase in pore-water pressure head). A decrease in water content during the drying process corresponded to an increase in matric suction (i.e., decrease in pore-water pressure head). The non-uniform changes in the pore-water pressure head profiles with respect to the elapsed time were due to the high nonlinearity of the SWCCs.

4.2. Barrier effect and effectiveness of the capillary barriers

"Capillary barrier effect" normally refers to the barrier effect produced by a coarser grained soil in impeding or reducing the downward movement of water through a soil system of a finer grained soil overlying a coarser grained soil. In this study, the barrier effect was demonstrated during the infiltration process and can be interpreted from the dis-

© 2004 NRC Canada

Fig. 12. Pore-water pressure head profiles in drawdown test in the soil column of fine sand over gravelly sand (FG-D).

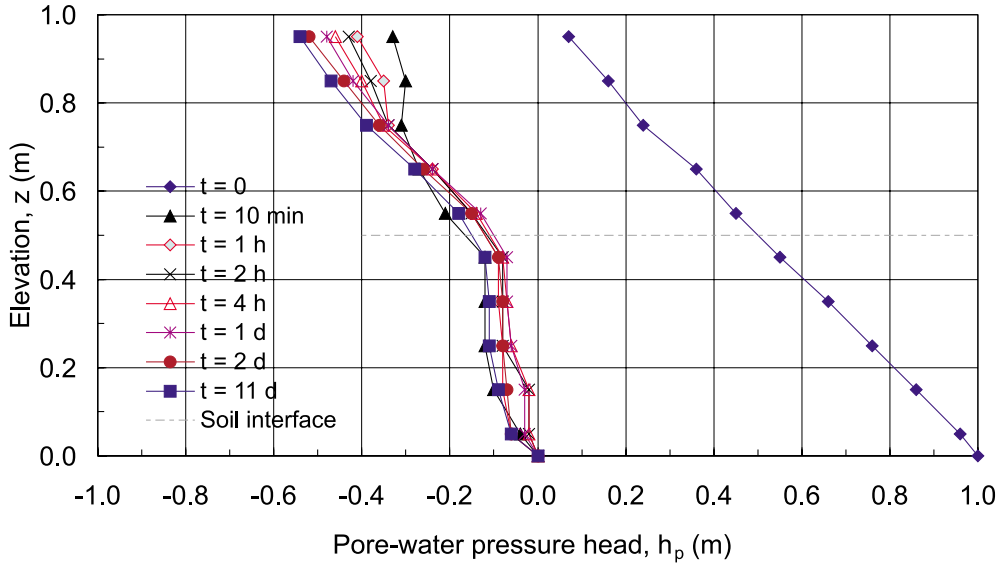

Fig. 13. Final volumetric water content in the soil column of medium sand over gravelly sand (at the end of rainfall test MG-R3) and fine sand over gravelly sand (at the end of rainfall test FG-R3).

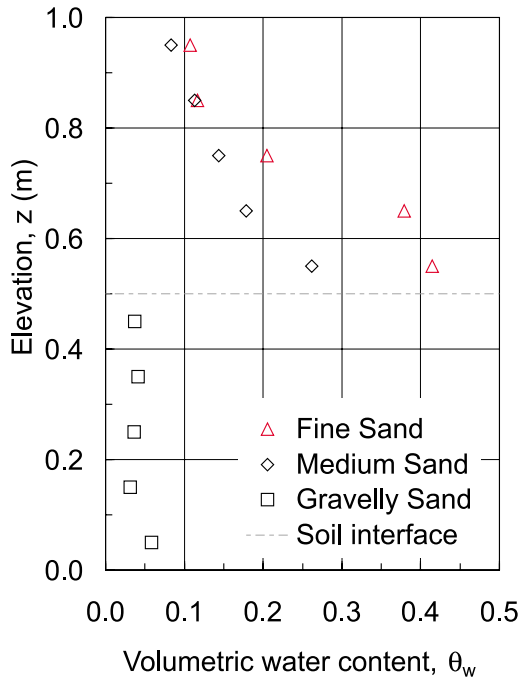

Table 3. Pore-water pressure head h_p (in m) across the soil interface in test FM-R2.

Elapsed time, t (h)	Fine sand (z = 0.55 m)	Coarse sand (z = 0.45 m)
0	–0.48	–0.42
2	–0.48	–0.42
4	–0.22	–0.42
6	–0.23	–0.20

tribution and change in the pore-water pressure head across the finer–coarser soil interface during the rainfall infiltration tests.

In soil column FM (e.g., test FM-R2 as shown in Fig. 7), at an elapsed time of 4 h, the pore-water pressure head above and below the soil interface was –0.22 and –0.42 m, respectively, as shown in Table 3. This indicated that the accumulated water in the finer layer near the soil interface resulted in a significant increase in the pore-water pressure head in the finer layer (i.e., 0.20 m higher than that of the coarser layer near the interface) in the first 4 h. In the first 4 h, infiltration occurred mainly in the finer layer but not in the coarser layer, as reflected by the fact that the pore-water pressure head remained unchanged in the coarser layer. In other words, the coarser layer served as a barrier and impeded the downward flow of water from the finer layer due to its relatively low pore-water pressure head and low k_w. This barrier effect resulted in a significant pore-water pressure head difference of 0.20 m (the actual value could be even higher than this value, as the nearest tensiometers were 0.05 m above and below the soil interface) that was sustained across the finer–coarser soil interface.

The barrier effect was not sustained for a long time when water content continued to increase in the finer layer. As a result, at an elapsed time of 6 h, the pore-water pressure head in the coarser layer near the interface (z = 0.45 m) increased by 0.22 m to a magnitude of –0.20 m (Fig. 7; Table 3). The change in pore-water pressure head in the finer layer near the interface was only 0.01 m between the elapsed time of 4 h and 6 h, however. The sudden increase in pore-water pressure head at z = 0.45 m indicated that during the period between 4 h and 6 h, water broke through the soil interface and flowed into the underlying coarser layer. Thus, the infiltration in the coarser layer was initiated and integrated with that of the finer layer. The capillary barrier was no longer effective after breakthrough occurred. After the rainfall stopped, the entire soil column became drier with time and the pore-water pressure head profile moved towards its ultimate equilibrium state.

© 2004 NRC Canada

In soil columns MG and FG, the barrier effect during a rainfall seemed to be less apparent than that in soil column FM with respect to the change in pore-water pressure head across the finer–coarser soil interface. For example, in test MG-R1 (Fig. 11), the pore-water pressure head in the coarser layer (i.e., the gravelly sand) was relatively high (with a minimum value about –0.10 m), and the pore-water pressure head profiles were far away from the hydrostatic line. As a result, the pore-water pressure heads in the finer layers near the soil interface in soil columns MG and FG were also relatively high during the rainfalls and relatively close to those in the underlying coarser layer.

The barrier effect was exhibited in a different way with respect to the water storage at the final stage of the drying process in the soil columns (i.e., Fig. 9 for column FM and Fig. 13 for columns MG and FG). In soil column FM, the volumetric water content in the finer layer (i.e., the fine sand) was much lower than that in the finer layers of soil columns MG and FG (i.e., the medium and fine sands, respectively). In columns MG and FG where the underlying coarser layers were the gravelly sand, the volumetric water contents in the finer layer just above the soil interface were close to their respective saturated volumetric water contents.

The previous discussion suggests that a capillary barrier had a temporary effect in restricting the downward movement of water, as evidenced by the change in pore-water pressure heads across the finer–coarser soil interface. When the rainfall was continuously applied to the soil surface, breakthrough at the soil interface would eventually occur under the one-dimensional condition. After the rainfall stopped, the pore-water pressures in the soils tended to develop towards the ultimate state following the drying process of the soils. In addition, the temporary barrier effect was more apparent in the case where the coarser layer was medium sand as compared to the case where the coarse layer was gravelly sand, even though both cases were under the same boundary conditions. This was due to the fact that medium sand had a higher water-entry value than gravelly sand, and the breakthrough at the finer–coarser soil interface occurred at a much higher matric suction head for the medium sand than for the gravelly sand. In terms of water storage in the finer layer at the final stage of the drying process, however, the capillary barrier with the coarser layer of gravelly sand was more effective in retaining water than that with the coarser layer of medium sand. The water storage in the finer layer appeared to be controlled by the soil type of the underlying coarser layer.

4.3. Water-entry value of the underlying coarse layer

The water-entry value of the coarser layer is defined as the matric suction at which water first moves into the smallest pores of the underlying coarser grained layer. Baker and Hillel (1990) termed this point the water-entry head. The water-entry values of the coarser grained layers used in this study can be estimated from the column test results.

In column FM (i.e., rainfall test FM-R2 in Fig. 7), water started to break through the finer–coarser interface and enter the underlying medium sand within the period between the elapsed times of 4 h and 6 h. Therefore, the matric suction at the finer–coarser interface during this period was the water-entry value of the medium sand. Since a matric suction profile must be continuous in soils, the water-entry value can be estimated by taking the average measurement of matric suctions across the soil interface at an elapsed time of 4 h when the breakthrough started to occur. The water-entry value of the medium sand in terms of head was 0.32 m ((0.42 + 0.22)/2, Table 3) when calculated using this method.

Baker and Hillel (1990) suggested that the water-entry value of a soil could be approximated to the height of capillary rise of the soil and could be estimated from the inflection point corresponding to the value of the residual matric suction on the drying SWCC. The residual matric suction of the medium sand was 3.75 kPa, as obtained from the drying SWCC (Table 2) (i.e., 0.375 m of matric suction head). From the wetting SWCC of the medium sand, the water-entry value can be deduced to be 0.318 m (3.18 kPa). Similarly, the water-entry value of the gravelly sand was estimated to be 0.05 m from rainfall test MG-R1 (Fig. 11) and 0.028 m (0.284 kPa) and 0.040 m (0.401 kPa) from the wetting and drying SWCCs, respectively. These observations support the suggestion from Baker and Hillel that the water-entry value of a soil is nearly equal to the residual matric suction value obtained from the drying SWCC of the soil. In addition, the water-entry values of the soils as observed from the rainfall tests were quite close to those determined from the wetting SWCC of the soil.

The water-entry value of the gravelly sand was much lower than that of the medium sand, and therefore the breakthrough at the finer–coarser soil interface occurred at a much lower matric suction head for the gravelly sand than for the medium sand. This suggests that the capillary barrier with the coarser layer of gravelly sand was more effective in restricting the downward flow of water from the overlying finer layer. This observation was in agreement with Stormont and Anderson (1999), who claimed that the more uniform and coarse the underlying soil layer, the more effective the layer would be as a capillary barrier.

4.4. Ultimate pore-water pressures in the capillary barriers

Water drained from the soil column continuously and the pore-water pressure head profiles moved towards the hydrostatic profile (or the equilibrium condition) when a constant water table was maintained at the bottom of the soil column (e.g., test FM-R2 in Fig. 7). This behaviour was observed in all infiltration tests either during the infiltration due to drawdown of the water table or during the percolation after rainfall had stopped. Before a hydrostatic condition was established, the pore-water pressure profile in the soil was located to the right of the hydrostatic profile (i.e., lower matric suction than that of the hydrostatic condition), and the total head in the soil varied from a positive value in the upper portion of the soil to zero at the water table. As a result, the hydraulic gradient was greater than zero and water tended to flow down continually. When pore-water pressures reached the hydrostatic state, the total head became zero throughout the soil column and the hydraulic gradient was equal to zero. At this state, no more water flow occurred in the soil column. Therefore, theoretically the pore-water pressure profile never stopped moving towards the hydrostatic profile until the hydrostatic condition was reached.

© 2004 NRC Canada

Fig. 14. Final pore-water pressure head profiles developed in soil columns FM, MG, and FG.

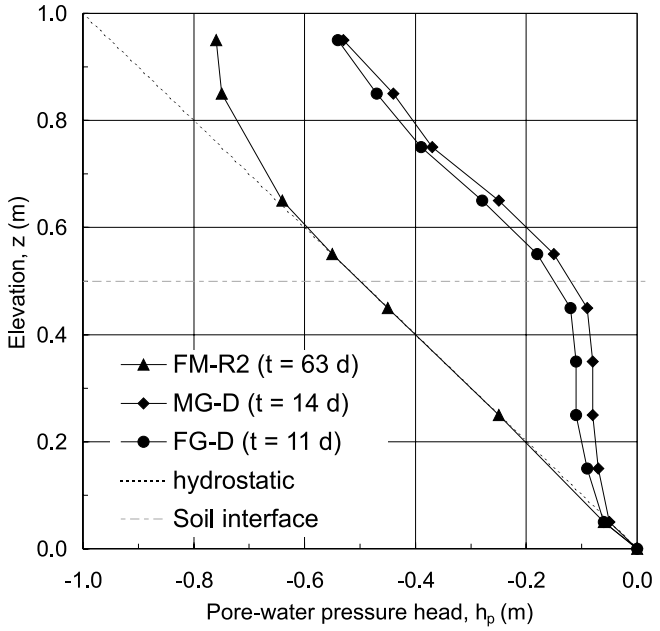

The test results showed, however, that the pore-water pressure profiles in soil columns FM, MG, and FG never quite reached the hydrostatic profile as illustrated in Fig. 14, where results of the tests with the longest drying time from each of the three soil columns are compiled. In test FM-R2, both the pore-water pressure (Fig. 7) and the drainage velocity (Fig. 8) changed at an extremely slow rate in the late stage of the drying process. This was particularly true at elapsed times greater than 40 days. The drainage velocity during the 11 days from day 52 to day 63 was estimated to be less than 1.9×10^{-11} m/s, as the weighing balance, with a resolution of 0.5 g, did not capture any change in the cumulative amount of drainage. This drainage velocity was also much smaller than the potential water evaporation rate in the laboratory (i.e., a value of 8.9×10^{-9} m/s as obtained from investigation). Therefore, after an elapsed time greater than 52 days, the development of the pore-water pressure head essentially stopped and there was essentially no drainage from the soil column (Fig. 8). The drying process lasted until an elapsed time of 63 days when the test was stopped. A similar process occurred during tests MG-D (Fig. 10) and FG-D (Fig. 12). The pore-water pressure profiles changed rapidly during the initial stage of the drying process (i.e., before an elapsed time of 2 days) and changed at an extremely slow rate after an elapsed time of 2 days. After an elapsed time of 6 days, there was essentially no change in pore-water pressure and drainage velocity, and therefore the drawdown tests were stopped after 14 and 11 days in tests MG-D and FG-D, respectively.

The observations that the pore-water pressure profiles in columns FM, MG, and FG could not reach a hydrostatic condition can be explained through the SWCCs and the permeability functions of the soils. At the initial stage of the drying process, the volumetric water content and k_w were relatively high and water could flow easily, resulting in a rapid change in pore-water pressures. As time elapsed, the volumetric water content and k_w became smaller and water in the soils likely changed into a discontinuous state. Since the flow of water relied on continuous channels in the soil which were filled with water, water was not able to flow when the water phase became discontinuous. In other words, k_w tended towards zero. The soil water was likely bound by the interparticle forces and the water was "locked" in the soil. This observation was consistent with that of Barbour and Yanful (1994) and Choo and Yanful (2000), in which similar non-equilibrium static conditions of pore-water pressure profiles were reported.

The maximum matric suction (or the lowest pore-water pressure) that could develop in a soil column can be estimated from the residual matric suction (ψ_r) of the soil, as it was noted that the maximum matric suction developed in a soil layer was close to the ψ_r value of the soil. The maximum matric suctions measured in the tests (Fig. 14) were 0.09 m for the gravelly sand (an average value from tests FG-D and MG-D), 0.54 m for the medium sand (test MG-D), and 0.76 m for the fine sand (test FM-R2). The ψ_r values for the gravelly sand, medium sand, and fine sand were 0.040 m (0.401 kPa), 0.375 m (3.750 kPa), and 0.394 m (3.940 kPa), respectively (Table 2). These results indicate that the maximum matric suctions developed in the soils were approximately one to two times the ψ_r values of the soils. Therefore, it could be suggested that, in extreme cases, the maximum possible matric suction in any soil in a soil column is about two times the residual matric suction of the soil (ψ_r). Barbour and Yanful (1994), however, suggested that the maximum possible matric suction is approximately the same as the matric suction corresponding to the residual water content.

The ultimate pore-water pressure profile in the soil can be estimated based on the maximum possible matric suction in the soil. For a single-layer soil column with a height greater than two times the residual matric suction (ψ_r) head of the soil, a hydrostatic pore-water pressure profile would develop from the water table to a height corresponding to two times the ψ_r head, which was then followed by a nearly vertical line, as demonstrated in the gravelly sand in tests MG-D and FG-D (Fig. 14). In a capillary barrier, the pore-water pressure head profile in the coarser layer will first develop to a maximum possible matric suction head equal to two times the ψ_r head of the coarser grained soil and then the profile will become a nearly vertical line up to the finer–coarser interface. The pore-water pressure head profile is continuous at the finer–coarser interface and develops further in the finer layer to the maximum possible matric suction head of the finer grained soil (approximately two times the ψ_r head of the finer grained soil). When the elevation height exceeds the maximum matric suction head of the finer layer, the pore-water pressure head will again become a vertical line. Therefore, an idealized possible ultimate pore-water pressure profile for a capillary barrier can be proposed as shown in Fig. 15, in which the maximum matric suction heads of the coarser and finer grained soils can be approximated by two times the residual matric suction heads of the respective soils. Figure 15 shows that the negative pore-water pressure profile can only develop to a limited extent in a capillary barrier. The proposed pressure head profile might be particu-

© 2004 NRC Canada

Fig. 15. Idealized possible ultimate pore-water pressure head and total head profiles in a capillary barrier.

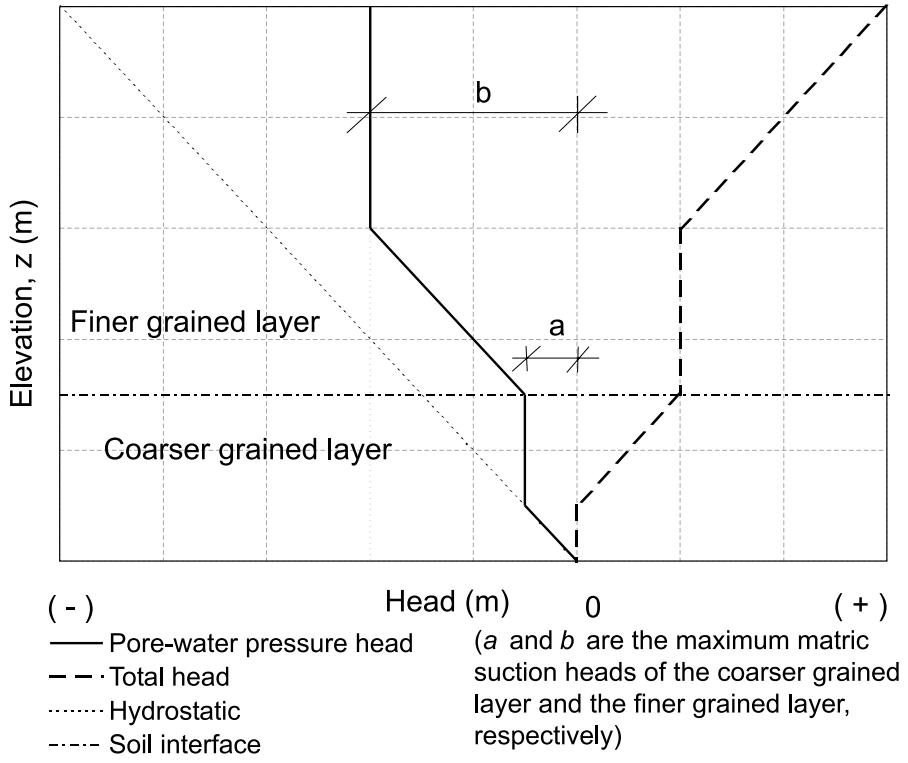

larly useful in estimating the negative pore-water pressure of a soil system when the water table is deep.

The previous discussion is based on the assumption that no evaporation and transpiration occurs from the soil column. The same condition applied to all the infiltration tests in the soil columns presented in this study. If there is evaporation or transpiration from the soil, the water content will further decrease and the pore-water pressure heads will further develop in the soil. Barbour and Yanful (1994) also suggested that only other mechanisms of water movement such as vapour flow could further decrease the negative pore-water pressure (i.e., increase the matric suction) when a non-equilibrium condition was developed.

4.5. Problems in the determination of drying SWCC using drying capillary rise open tube

The capillary rise open tube was used to investigate the wetting SWCC of the soils used in this study. Similarly, the capillary rise open tube test can also be used to investigate the drying SWCC where the soil in the tube is initially saturated and subsequently dried. During the wetting or drying process of the capillary tube test, no evaporation or transpiration is allowed. At the end of the test, the water content of the soil at different elevations can be measured. The elevation heads can be converted to pressure heads and subsequently to the matric suction of the soil. The plot of water content against matric suction can be obtained from the wetting and drying capillary tube tests to give the wetting and drying SWCCs.

The capillary rise open tube method to determine the drying SWCC presumes that the elevation head is equal to the negative pore-water pressure head (i.e., the soil in the tube is under a hydrostatic equilibrium condition with respect to the water table at the bottom of the soil tube). Lambe and Whitman (1979) also stated that, for the static equilibrium state, the pore-water pressure at any point in the soil in such an open tube is exactly equal to the height of the point above the phreatic line multiplied by the unit weight of water. The results of the infiltration tests from the soil columns and the earlier discussions, however, suggest that this assumption is conditional.

The test results from columns FM, MG, and FG show that the pore-water head profile may not reach the hydrostatic condition (Fig. 14). This indicates that under these non-equilibrium conditions, the actual pore-water pressures in the soil above the point where the pore-water pressure head starts to deviate from the hydrostatic line are smaller than the hydrostatic pore-water pressures. The pore-water pressure is equal to the elevation height multiplied by the unit weight of water only for points below the starting point of the deviation from the hydrostatic condition. The starting point of the deviation from the hydrostatic condition can be approximated as two times the residual matric suction head of the soil, as discussed in the previous section, and the residual suction can be measured by another method (i.e., pressure plate test). This further suggests that the drying capillary tube method can only be used to establish the drying SWCC of a soil up to a matric suction equal to two times the residual matric suction of the soil. This condition applies because the matric suction will not develop beyond two times the residual matric suction of the soil, at least not within a reasonable time scale.

© 2004 NRC Canada

Fig. 16. Comparison of the final volumetric water content versus matric suction of the gravelly sand in the soil columns with the fitted SWCCs.

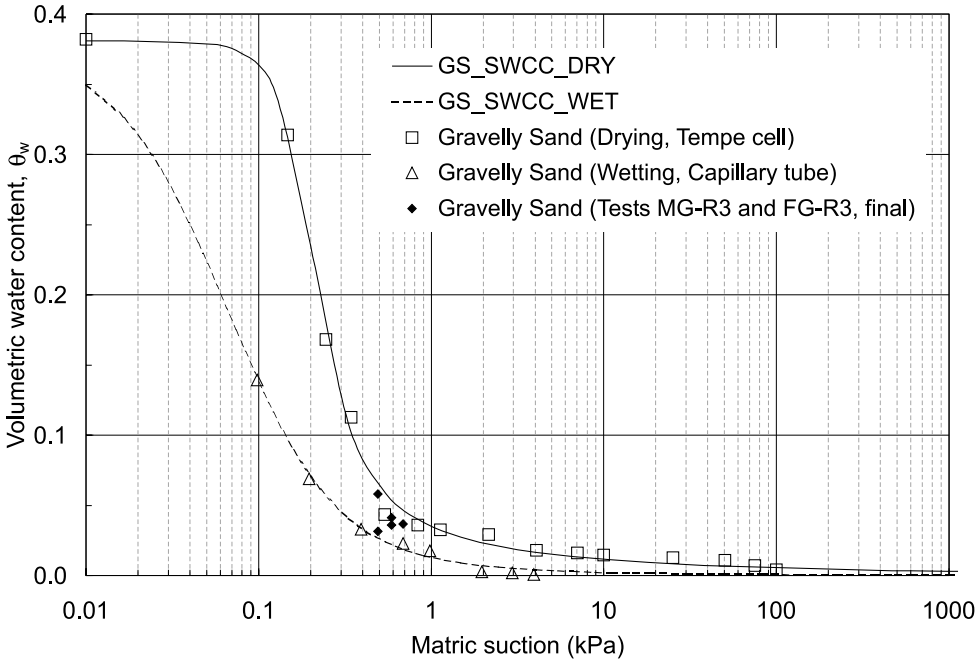

Fig. 17. Comparison of the final volumetric water content versus matric suction of the medium sand in the soil column with the fitted SWCCs.

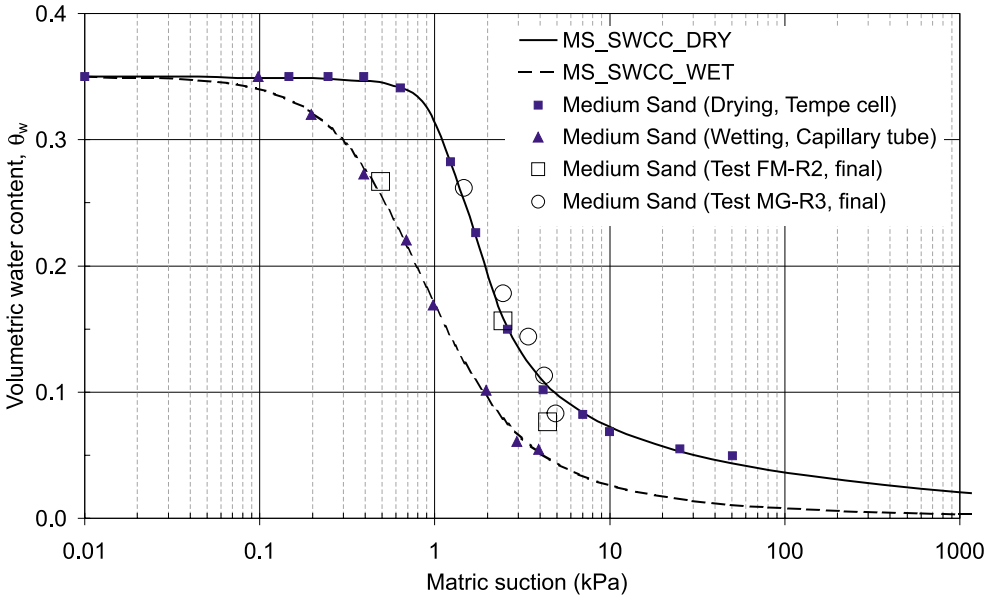

4.6. Final volumetric water contents versus matric suctions in the soils

The final volumetric water contents of the soils in each soil column were measured using the oven-drying method. The results, together with the matric suctions converted from the pore-water pressure heads as measured using tensiometers, were plotted and compared with the fitted SWCC for each soil (i.e., Fig. 16 for the gravelly sand, Fig. 17 for the medium sand, and Fig. 18 for the fine sand).

The comparison showed that there was reasonable consistency between the results of the soil column test and the fitted SWCC. The results from the medium sand and the fine sand were close to the drying SWCC for the respective soils, since the results were obtained after a drying process in the soil columns. The results of the gravelly sand were rather close to the residual matric suction of 0.4 kPa, which was reasonably consistent with the observation that the maximum matric suction developed in the soil column was less than 0.9 kPa (final measured value is about 0.7 kPa, see Fig. 16). These results also suggest that the drying SWCC of

© 2004 NRC Canada

Fig. 18. Comparison of the final volumetric water content versus matric suction of the fine sand in the soil column with the fitted SWCCs.

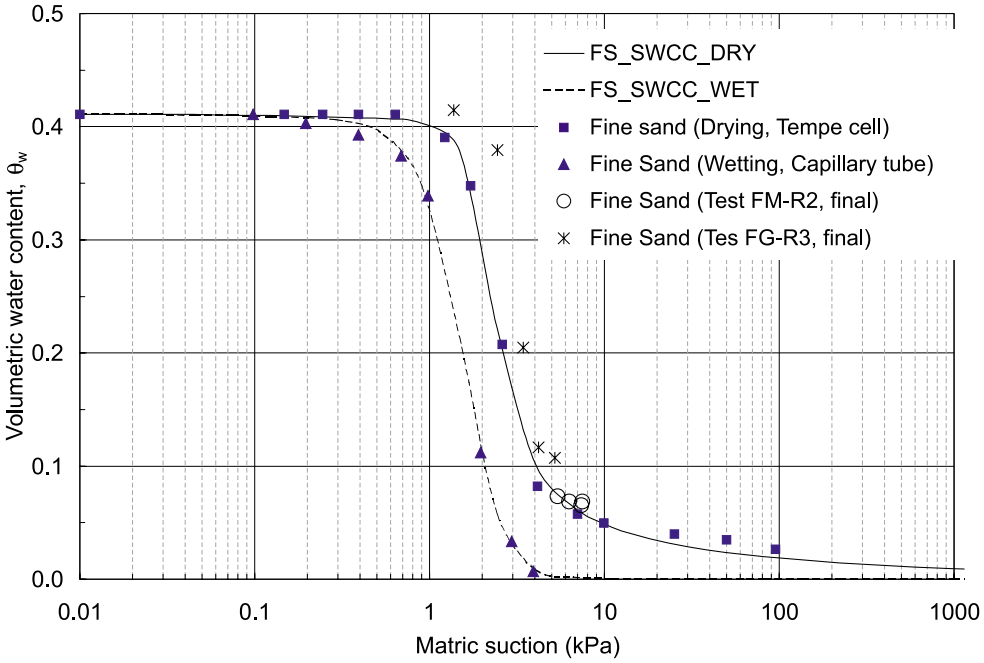

a soil can be obtained through the use of a drying soil tube by measuring both its volumetric water content and matric suction, provided the height of the column is less than two times the residual matric suction head of the soil, as discussed earlier.

5. Conclusions

Infiltration tests were conducted on three capillary barriers of fine sand over medium sand, medium sand over gravelly sand, and fine sand over gravelly sand. The capillary barrier effect was clearly shown in the underlying coarser soil layer. The barrier effect was more apparent when using the coarser layer of medium sand than when using the coarser layer of gravelly sand, in terms of the pore-water pressure change across the finer–coarser soil interface, especially when breakthrough occurred. The more apparent barrier effect when using the medium sand can be attributed to the fact that the coarser layer of medium sand could develop a lower pore-water pressure head initially than the coarser layer of gravelly sand. In terms of the final water storage in the finer layer, however, the barrier effect was more obvious when using the coarser layer of gravelly sand, and this was possibly due to the lower permeability developed in the gravelly sand. In principle, the capillary barrier comprising the coarser layer of gravelly sand was more effective than the capillary barrier comprising the coarser layer of medium sand because the gravelly sand had a lower water-entry value. In other words, the more uniform and the coarser the texture of a soil, the more effective the soil will be at forming a capillary barrier. In addition, the water-entry value of the coarser layer, at which breakthrough occurs, is approximately equal to the residual matric suction of the coarser layer.

Capillary barriers are only effective temporarily under a one-dimensional, vertical flow condition, as water tends to break through the soil interface sooner or later and flow through the coarser layer. The pore-water pressure profile tends to move towards the ultimate pressure profile during the drying stage after rainfall is stopped. The ultimate pore-water pressure profile is not a hydrostatic profile if the soil column is higher than two times the residual matric suction head of the finer soil layer. The ultimate pore-water pressure profile can also be estimated from the residual matric suctions of the soils as proposed in this paper. As a result of the possible non-equilibrium condition developed in the capillary rise open tube or soil column, the drying SWCC of a soil can be obtained from the drying capillary rise open tube or the drying soil column only for a matric suction range lower than two times the residual matric suction of the soil.

The proposed ultimate negative pore-water pressure profile can be used to evaluate the maximum possible matric suction in a soil and to estimate the water content in the soil using the available SWCC for the soil under a condition of zero or relatively low evaporation or transpiration.

Acknowledgments

The authors gratefully acknowledge the financial assistance provided by the Nanyang Technological University, Singapore, for this research work under RG 7/99, Capillary barrier for slope stabilization, and ARC 12/96, Development of an instrument for field measurement of suction in unsaturated soil. The first author acknowledges the research scholarship received from the Nanyang Technological University, Singapore.

© 2004 NRC Canada

References

ASTM. 1997*a*. Standard test method for particle-size analysis of soils (D422-63). *In* Annual Book of ASTM Standards, sect. 4, vol. 04.08. American Society for Testing and Materials (ASTM), Philadelphia, Pa. pp. 10–16.

ASTM. 1997*b*. Standard test method for specific gravity of soils (D854-92). *In* Annual Book of ASTM Standards, sect. 4, vol. 04.08. American Society for Testing and Materials (ASTM), Philadelphia, Pa. pp. 88–91.

ASTM. 1997*c*. Standard test method for permeability of granular soils (constant head) (D2434-68). *In* Annual Book of ASTM Standards, sect. 4, vol. 04.08. American Society for Testing and Materials (ASTM), Philadelphia, Pa. pp. 202–206.

ASTM. 1997*d*. Standard classification of soils for engineering purposes (unified soil classification system) (D2487-93). *In* Annual Book of ASTM Standards, sect. 4, vol. 04.08. American Society for Testing and Materials (ASTM), Philadelphia, Pa. pp. 217–227.

ASTM. 1997*e*. Standard test method for capillary-moisture relationships for coarse- and medium-textured soils by porous-plate apparatus (D2325-68). *In* Annual Book of ASTM Standards, sect. 4, vol. 04.08. American Society for Testing and Materials (ASTM), Philadelphia, Pa. pp. 195–201.

Baker, R.S., and Hillel, D. 1990. Laboratory tests of a theory of fingering during infiltration into layered soils. Soil Science Society of America Journal, **54**: 20–30.

Barbour, S.L., and Yanful, E.K. 1994. A column study of static nonequilibrium fluid pressure in sand during prolonged drainage. Canadian Geotechnical Journal, **31**: 299–303.

Choo, L.P., and Yanful, E.K. 2000. Water flow through cover soils using modeling and experimental methods. Journal of Geotechnical and Geoenvironmental Engineering, ASCE, **126**(4): 324–334.

Fredlund, D.G., and Rahardjo, H. 1993. Soil mechanics for unsaturated soils. John Wiley and Sons, Inc., New York.

Fredlund, D.G., and Xing, A. 1994. Equations for the soil-water characteristic curve. Canadian Geotechnical Journal, **31**: 521–532.

Fredlund, D.G., Xing, A., and Huang, S. 1994. Predicting the permeability function for unsaturated soils using the soil-water characteristic curve. Canadian Geotechnical Journal, **31**: 533–546.

Lambe, T.W. 1951. Soil testing for engineers. John Wiley and Sons, Inc., New York.

Lambe, T.W., and Whitman, R.V. 1979. Soil mechanics. SI Version. John Wiley and Sons, Inc., New York. pp. 245–246.

Ross, B. 1990. The diversion capacity of capillary barriers. Water Resources Research, **26**(10): 2625–2629.

Soilmoisture Equipment Corporation. 1999. Catalogue. Soilmoisture Equipment Corporation, Santa Barbara, Calif.

SoilVision Systems Ltd. 1997. SoilVision. Version 1.31. User's manual. SoilVision Systems Ltd., Saskatoon, Sask.

Stormont, J.C. 1996. The effectiveness of two capillary barriers on a 10% slope. Geotechnical and Geological Engineering, **14**: 243–267.

Stormont, J.C., and Anderson, C.E. 1999. Capillary barrier effect from underlying coarse soil layer. Journal of Geotechnical and Geoenvironmental Engineering, ASCE, **125**(8): 641–648.

Yanful, E.K., Ridley, M.D., Woyshner, M.R., and Duncan, J. 1993. Construction and monitoring of a composite soil cover on an experimental waste-rock pile near Newcastle, New Brunswick, Canada. Canadian Geotechnical Journal, **30**: 588–599.

© 2004 NRC Canada